

Published in final edited form as:

Cancer Res. 2010 September 15; 70(18): 7273–7282. doi:10.1158/0008-5472.CAN-10-1142.

Using the Transcription Factor Inhibitor of DNA Binding 1 to Selectively Target Endothelial Progenitor Cells Offers Novel Strategies to Inhibit Tumor Angiogenesis and Growth

Albert S. Mellick^{1,*}, Prue N. Plummer¹, Daniel J. Nolan², Dingcheng Gao², Kathryn Bambino², Mary Hahn², Raul Catena², Vivian Turner³, Kevin McDonnell², Robert Benezra⁴, Robert Brink³, Alexander Swarbrick³, and Vivek Mittal^{2,*}

¹School of Medical Science, Griffith University, Gold Coast, Queensland, Australia

²Weill Cornell University Medical College, New York, New York

³Garvan Institute of Medical Research, Sydney, Australia

⁴Program in Cancer Biology and Genetics, Memorial Sloan-Kettering Cancer Center, New York, New York

Abstract

Tumor angiogenesis is essential for malignant growth and metastasis. Bone marrow (BM)-derived endothelial progenitor cells (EPCs) contribute to angiogenesis-mediated tumor growth. EPC ablation can reduce tumor growth, however, the lack of a marker that can track EPCs from the BM to tumor neovasculature has impeded progress in understanding the molecular mechanisms underlying EPC biology. Here, we report the use of transgenic mouse and lentiviral models to monitor the BM-derived compartment of the tumor stroma; this approach exploits the selectivity of the transcription factor inhibitor of DNA binding 1 (Id1) for EPCs to track EPCs in the BM, blood, and tumor stroma, as well as mature EPCs. Acute ablation of BM-derived EPCs using Id1-directed delivery of a suicide gene reduced circulating EPCs and yielded significant defects in angiogenesis-mediated tumor growth. Additionally, use of the Id1 proximal promoter to express miR-30 based short hairpin RNA inhibited expression of critical intrinsic EPC factors, confirming that signaling through VEGFR2 is required for EPC mediated tumor biology. By exploiting the selectivity of Id1 gene expression in EPCs, our results establish a strategy to track and target EPCs *in vivo*, clarifying the significant role that EPCs play in BM-mediated tumor angiogenesis.

Keywords

Bone Marrow Transplantation; Inhibitor of DNA Binding 1; Endothelial Progenitor Cells; Angiogenesis; Short Hairpin RNA Inhibition

Introduction

The tumor microenvironment is composed mainly of bone marrow (BM)-derived cells, which are critical to angiogenesis-mediated tumor growth and spread (1). These include

*Requests for reprints: Albert S. Mellick, School of Medical Science, Griffith University, Parklands Dr, Gold Coast, QLD 4215, Australia. a.mellick@griffith.edu.au or Vivek Mittal, Weill Cornell University Medical College, 525E 68th St, 1300 York Ave New York, NY 10021, USA. vim2010@med.cornell.edu.

Disclosure of Potential Conflicts of Interest: No potential conflicts of interest were disclosed.

myeloid cells such as Tie-2⁺ and GR-1⁺ monocytes (2–5), tumor associated macrophages (6,7), inflammatory cells (8,9), PDGFR β ⁺ pericytes (10) and endothelial progenitor cells (EPCs) (11–13). Of particular interest are the BM-derived EPCs, as they have been demonstrated to play a significant role in the growth of early tumors and metastatic lesions by mediating the angiogenic switch (14–17). EPCs have also been proposed to provide an alternative source of tumor endothelium, which contribute to neovessel formation by directly incorporating into nascent vasculature as differentiated endothelial cells (11–13). Therefore, EPCs represent important new targets for novel antiangiogenic therapies without the side-effects associated with current therapies, which also target host vasculature (14–17).

EPCs are detected as a unique cell population in the peripheral blood (PB), expressing a variety of cell surface markers, which identify them as vascular and BM-derived. Key EPC markers include Vascular Endothelial (VE)-Cadherin, Vascular Endothelial Growth Factor Receptor (VEGFR) 2, CD31^{low}, c-kit and Prominin 1/AC133 (16–19). However, the expression of these markers differs depending on whether the EPCs are in the BM, PB or tumor. This lack of a single marker to be able to unambiguously track EPCs has led to several recent cancer studies failing to identify EPCs in specific mouse tumor models (18–21). This has also raised concerns as to whether the same population is being truly monitored *in vivo*, and has imposed tremendous limitations upon the assessment of the biological function of tumor associated EPCs, as well as, their potential as targets for antiangiogenic cancer therapy.

Previous studies have demonstrated that like tumor-activated endothelium, BM-EPCs also express the Inhibitor of DNA Binding 1 (Id1). Id1 is a member of the helix-loop-helix family of transcription factors and a marker of self renewal (22). We have previously shown that global inhibition of Id1 in the BM results in significant specific EPC-linked tumor vascular defects (17,23). These findings nominate Id1 as a potential marker of EPCs.

The aims of this study were to determine if Id1 could be used to track EPCs *in vivo*, specifically target EPCs and modify EPC mediated tumor growth. Using a knock-in Id1 reporter mouse (24) and lentiviral (LV) transduction of BM transplanted (BMT) into wild type (WT) recipients, we have demonstrated that Id1 gene activity can be used to track and modify BM-EPCs in the BM, blood, BM compartment of the tumor-stroma; as well as luminally incorporated BM-EPCs. Furthermore, selective ablation of EPCs *in vivo*, using the Id1 proximal promoter (pr/p) to drive the expression of the suicide gene herpes simplex virus (HSV)-Thymidine Kinase (*tk*), resulted in specific EPC-linked vascular defects, and impaired tumor growth. Directed delivery of short hairpin RNA inhibition (shRNAi) by the LV-Id1pr/p was also used to inhibit key EPC linked factors, such as VEGFR2; resulting in marked EPC and angiogenesis linked tumor growth defects. This work underscores the functional importance of EPCs to tumor biology, and directly links EPC-intrinsic Id1 to EPC biology and EPC mediated tumor vascular growth. It also demonstrates that EPCs represent a unique lineage that can be tracked from BM to tumor using Id1.

Materials and Methods

Mice

WT C57BL/6 mice, C57BL/6 Id1^{+/GFP} transgenic reporter mice (24), and green fluorescent protein (GFP) transgenic C57BL/6-Tg (ACTb-EGFP) 10sb/J mice expressing GFP under a hybrid chicken β -actin promoter and cytomegalovirus intermediate early enhancer (25) were purchased from The Jackson Laboratory. All procedures involving mice were conducted in accordance with protocols reviewed and approved by institutional animal care and ethics committees.

Cell lines and growth conditions

Murine Lewis lung carcinoma (LLC) cells/D122 (provided by Lea Eisenbach, Wiesmann Institute of Science, Israel), murine lymphoma cells B6RV2 (14), and murine endothelial cells (mHEVc; provided by J. Cook-Mills, University of Cincinnati, Cincinnati, OH; ref. 26) were maintained in RPMI with 15% FBS. Murine myoblast progenitors C2C12 cells (ATCC) and human kidney 293T cells were maintained in DMEM supplemented with 10% FCS.

Screening shRNAs

ShRNAs targeting Id1 were cloned into a U6 or Id1 promoter-containing vector as described (27). shRNA, targeting firefly luciferase served as a non-specific control. SYBR Green I detection (28) was used for RT-PCR analysis using the ABI7700 real time PCR detection system (Applied Biosystems). Primers for RT-PCR analysis: VEGFR2 (*forward*: 5'-ATCGTGTACATCACCGAGAACA-3' and *reverse* 5'-CGGCATAGCTGATCATGTAAC T-3'); Id1 (*forward*: 5'-GTACTTGGTCTGTCGGAGCAA-3' and *reverse*: 5'-CATGTCGTAGAG CAGGACGTT-3'). Internal controls: β -actin (*forward* 5'-TGTTTGAGACCTTCAACACC-3' and *reverse*: 5'-TAGGAGCCAGAGCAGTAATC-3') or GAPDH (*forward*: 5'-TCAACGACCCTTCATTGAC-3' and *reverse*: 5'-ATGCAGGGATGATGTTCTGG-3').

Generation of LV constructs

To generate pWPT- Ω , a gateway destination cassette ccdB (Invitrogen) was inserted into the *SalI* site in the LV pWPT (D. Torono, University of Geneva, Geneva, Switzerland), and shRNAs were transferred from shuttle vectors by gateway recombination. To generate Id1pr/p-GFP LV a 1.32kb fragment containing the murine proximal Id1 promoter was amplified from C57BL/6 mouse genomic DNA and inserted into the pWPT-LV, replacing the EF1 α -short promoter. To create Id1pr/p-RFP, GFP was replaced (*MluI/XhoI*) with monomeric Red Fluorescent Protein (mCherry; ref. 29). To generate pWPT-Id1pr/pGFPITK, the HSV-*tk* gene was amplified from pSHTK (Provided by Ventura, Universidade de São Paulo, City of São Paulo, São Paulo, Brasil), and inserted downstream of GFP/RFP, and an internal ribosome entry site (IRES; provided by Patrick Paddison, Cold Spring Harbor Laboratories, City of Cold Spring Harbor, United States of America). MicroRNA-30 (miR-30) based shRNA were amplified from shuttle vectors and cloned downstream of GFP.

LV production, BM transduction and transplantation

LV pseudotyped with the vesicular stomatitis G protein (VSVG) were generated by Calcium Phosphate transfection into 293T cells with three packaging constructs, pMDLg/pRRE, REV and pVSVG as described (30). Viral titer was determined by p24 ELISA (Perkin Elmer) or Fluorescence-activated cell sorting (FACS) analysis of LV-infected 293T cells in the presence of serum. LV transductions of lineage-depleted BM cells (multiplicity of infection of ~50) were performed in serum-free StemSpan SFEM medium (Stem Cell Technologies) in the presence of interleukin-3 (IL-3; 20 ng/mL), IL-6 (100 ng/mL), and stem cell factor (100 ng/mL) for 12 h. For BMT, 5×10^5 lineage depleted BM cells were injected into the tail veins of lethally irradiated (1100rads) C57BL/6 mice. Following BMT, RT-PCR analysis was used to determine transduction efficiency of LV infected BM cells. DNA was isolated from the BM, and subjected to RT-PCR using GFP specific primers: *forward*: 5'-GCTCTGCCCTCTCATTGTACA-3' and *reverse* 5'-GTGAACAGCTCCTCGCCCTT-3'. A standard curve was generated from titrated target DNA and vector copy number determined.

Analysis of tumors, blood and bone marrow by immunohistochemistry and microscopy

C57BL/6 mice were inoculated intradermally with 5×10^6 LLC or B6RV2 cells and tumor size was monitored, and analyzed by microscopy (16). For circulating endothelial progenitors (CEP) analysis tail blood was collected in anti-coagulant buffer (PBS, 5mM EDTA) and for BM-EPC analysis BM was flushed from the bones. PB mononuclear cells (PBMNCs) and BM mononuclear cells (BMMNCs) were isolated by gradient centrifugation using Histopaque 1077 (Sigma) and then either cytopun onto Superfrost slides or stained for FACS analysis. Primary antibodies, CD31/PECAM-1 (clone MEC 13.3), VE-Cadherin/CD144 (clone 11D4.1), CD11b (clone M1/70), VEGFR2/Flk1 (clone avas12 α 1), GR-1 (clone RB6-8C5), pan CD45 (clone 30-F11), B220 (clone RA3-6B2), CD3 (clone 500A2), c-kit/CD117 (clone 2B8), TIE2 (clone 33), TER-119 (clone TER-119) were obtained from BD Pharmingen, and Prominin 1 (clone 13A4) from eBiosciences, and Ki-67 (clone SP6) from NeoMarkers. Unless otherwise stated EPCs/CEPs were selected as a VE-Cadherin⁺, VEGFR2⁺, c-kit⁺, CD45⁻, CD11b⁻ subpopulation isolated by FACS from the mononuclear population in the BM/blood. Myeloid populations were selected as CD11b⁺ (myeloid cells) and either GR-1⁺ (neutrophils), Tie-2⁺ (Tie-2⁺ monocytes), B220⁺ (B cells), or CD3⁺ (T cells), and isolated by FACS from the mononuclear population in the blood or BM. All populations are negative for TER119 (Erythroid marker).

Microscopy was performed using 30 μ m sections, stained with Alexa-fluor conjugated primary antibodies with DAPI staining for cell nucleus (Invitrogen). In some cases, Alexa-fluor conjugated secondary anti-rabbit antibodies were used for staining with anti-Id1 monoclonal antibody (22). RFP/GFP⁺ cells were detected by their own signal. Fluorescent images were obtained using a Zeiss fluorescent microscope, (Software Axiovision LE 4) resolutions of 0.275–0.35 μ m as described (16).

FACS analysis

Single-cell suspensions were preblocked with F_c block (CD16/CD32, BD Pharmingen) and incubated with primary antibodies: IgG2 α κ and IgG2 α β isotype controls, and various antibodies described previously. Labeled cells were measured by LSRII flow cytometer (Beckton Dickinson), compensation by FACS Diva software (BD Immunocytometry Systems). Animals were also injected with Alexa Fluor 647 conjugated Isolectin GS-IB₄ (50 μ g for 10min, Molecular Probes) before sacrifice. Multivariate FACS was performed using isotype antibodies, fluorescence-minus-one samples, and unstained samples for determining appropriate gates, voltages, and compensation (31).

Statistics & data analysis

Statistical analysis was performed using GraphPad Prism™ Software (version 3.0). Statistical analysis of tumor growth one-way ANOVA ($\alpha=0.05$) was used to compare different treatments. For comparison of groups at end point Student's t-Test analysis ($\alpha=0.05$) was used. Unless otherwise stated data is presented as mean \pm standard error of the mean (SEM).

Results

Id1 is up-regulated in BM and tumor associated EPCs

Gene expression profiling showed that Id1 was one of several genes significantly up-regulated at least 4-fold in BM stem cells obtained from tumor challenged mice (Supplementary Fig. S1A). As Id1 knockout mice exhibit impaired EPC linked angiogenic and tumor growth defects (14, 19), we next determined to localize Id1 to specific BM-derived cell populations in the tumor-stroma. To do this we transplanted BM from β -actin (ACTb)-EGFP mice (25) into irradiated age-matched, syngeneic, WT recipients, and

examined pre-angiogenic, as well as vascularized, tumors following intradermal inoculation of LLC cells. Notably, Id1 protein was confined to BM-derived GFP⁺ VE-Cadherin⁺ EPCs (16), and not to other BM-derived GFP⁺ myeloid cells (Supplementary Fig. S1B).

The Id1 gene activity marks EPCs in the BM, blood and tumor stroma

To determine whether a genetic strategy using the Id1 gene activity might be used to track EPCs and investigate EPC function *in vivo*, the proximal promoter (pr/p) of Id1 (1.32kb), containing known Id1 regulatory sequences (32), and driving fluorescent reporter genes (GFP and RFP/mCherryTM), were cloned into the pWPT, self-inactivating LV vector (29) (Fig. 1A, B, Upper). The functionality of the Id1pr/p constructs was confirmed after stable transduction. In this experiment dose-dependent enhancement of reporter activity was observed, following administration of serum (not shown), or growth factors, to cells lines stably transduced with the LV-Id1pr/p constructs (Supplementary Fig. S2A).

To evaluate the selectivity of Id1pr/p for EPCs *in vivo*, BM cells not yet expressing key lineage markers (lineage depleted BM, see Methods), obtained from WT mice were transduced with Id1pr/p-GFP *ex vivo*, and transplanted into irradiated WT recipients. To determine the relative abundance of EPCs with respect to other BM-derived cells, lineage depleted BM cells derived from ACTb-EGFP⁺ mice were also transduced with LV-Id1pr/p-RFP. Following BM engraftment, RT-PCR analysis showed an average of 2–4 LV integrations per cell (Supplementary Fig. S2B). Id1pr/p-GFP/WT and Id1pr/p-RFP/ACTb-EGFP⁺ BMT animals were then LLC tumor challenged. Analysis of early tumors (day 6–8) showed recruitment of Id1pr/p-GFP/RFP⁺ VE-Cadherin⁺ cells to the tumor periphery (Fig. 1A, B, Lower). In addition to VE-Cadherin, these cells also expressed other EPC markers (16), including VEGFR2 and Prominin 1 (Supplementary Fig. S3A, B). Furthermore, none of these Id1pr/p⁺ cells expressed the myeloid marker CD11b, thus supporting these cells are EPCs (Supplementary Fig. S3C). In the blood, reporter analysis showed that the majority of VEGFR2⁺ c-kit⁺ CD11b⁻ CEPs (80%, $P < 0.001$) were Id1pr/p⁺; while BM hematopoietic cells of the myeloid lineage expressed negligible levels of Id1pr/p activity (0.09%, $P < 0.001$) (Supplementary Fig. S4A, B; Supplementary Table S1). Additionally, analysis of the BM showed that Id1pr/p activity was restricted to VE-Cadherin⁺ CD11b⁻ cells (66.83%, $P < 0.001$), thus supporting the Id1pr/p is marking EPCs (Supplementary Fig. S4C; Supplementary Table S1). Finally, the Id1pr/p⁺ cells also expressed endogenous Id1 protein in the blood, BM and tumor-stroma (Fig. 1C).

To confirm that we had captured the important regulatory regions in the LV constructs used and to determine whether the observed effects were due to positional effects or chromosomal positioning of the LV vector, we took advantage of the recently available Id1^{+/GFP} knock-in fluorescent reporter mice (24). In this experiment, BM from these mice was transplanted into irradiated WT mice and tissues examined in the context of LLC tumor challenge. In confirmation of the LV work, GFP activity was exclusively restricted to VE-Cadherin⁺ CD31^{low} CD11b⁻ BM-derived cells (EPCs) in the tumor-stroma of early tumors (Fig. 1D & 2A Upper).

The Id1 gene activity marks mature EPCs incorporated as part of functional tumor vasculature

Analysis of later tumors (day 8–12) from LV and Id1^{+/GFP} BMT mice revealed luminally incorporated GFP⁺ CD31⁺ CD11b⁻ mature EPCs in a subset of tumor neovessels (Fig. 2A Lower, B, Supplementary Fig. S5A, B). This demonstrates that the Id1pr/p also marks mature EPCs incorporated as endothelial cells (16). We next quantified these luminally incorporated BM-derived Id1⁺ endothelial cells by FACS following administration of Isolectin GS-IB4 (16). Of the total functional vasculature, as determined by lectin⁺ CD31⁺

CD11b⁻ cells, $9.4 \pm 2.6\%$ of the vessel-incorporated luminal endothelial cells (GFP⁺ lectin⁺ CD31⁺ CD11b⁻) at day 8 were BM-derived and expressed the Id1pr/p (Fig. 2C, D).

Ablation of Id1⁺ cells results in angiogenesis inhibition and impaired tumor growth

To determine the biological function of EPCs in tumor angiogenesis and to accomplish selective EPC ablation, the Id1pr/p-LV was used to express the suicide gene, HSV-*tk* (33) (Fig. 3A Upper, Supplementary Fig. S6A–C). This was done by transducing lineage depleted BM cells with the LV-Id1pr/p-GFPITK and transplanting these cells into irradiated WT recipients. The administration of Ganciclovir (GCV) showed a significant delay in tumor growth in Id1pr/p-GFPITK mice (~70%, by day 20) compared with controls (Fig. 3A Lower).

FACS analysis showed that the GCV treatment resulted in a ~3-fold reduction in CEPs in PB of Id1pr/p-GFPITK mice (Fig. 3B). As there was no significant change in other BM-derived hematopoietic cells, or progenitors it can be concluded this reduction was CEP specific (Fig. 3B). We next sought to determine whether this reduction in CEPs was due to *tk*-mediated BM-EPC ablation. Analysis of BM showed a >2-fold reduction in EPCs, with no significant reduction in CD11b⁺ hematopoietic cells in Id1pr/p-GFPITK (+GCV) mice (Fig. 3C). In concordance with this observation, actively proliferating EPCs were observed in tumor challenged BM as judged by Ki-67 staining (34) (Supplementary Fig. S6D). The Id1pr/p-GFPITK (+GCV) tumors also showed a significant reduction in vessel density and growth as compared with untreated Id1pr/p-GFPITK controls (Fig. 3D, $P < 0.0001$). These results demonstrate that Id1pr/p mediated delivery of *tk*, while resulting in the selective elimination of EPCs, appeared to also be associated with limited bystander effects; a complicating factor in many GCV/*tk* based approaches (35).

Id1 directed silencing of EPC-intrinsic factors results in inhibition of angiogenesis mediated tumor growth

To determine whether EPC-intrinsic factors such as Id1 and VEGFR2 were required for EPC-mediated tumor angiogenesis, and whether Id1 ablation specifically affected EPC biology in the context of tumor challenge, we used short hairpin (Ω) RNA inhibition, delivered by the LV-Id1pr/p construct to directly inhibit BM-EPCs. Firstly, to assess lentiviral mediated shRNA delivery *in vivo*, vectors with the constitutive U6 promoter driving RNAi were used (Supplementary Fig. S7A, B Upper). As expected from the EPC-linked tumor angiogenesis defects observed in Id1 knockout mice (14), BM-wide suppression of Id1 resulted in impaired B6RV2 lymphoma (Supplementary Fig. S7B, Lower Right) and LLC (Supplementary Fig. S7B, Lower Left) tumor growth. This finding was associated with reduced tumor vascularization and Id1mRNA suppression (Supplementary Fig. S7C, D).

To facilitate expression by the polII Id1 promoter, miR-30-based shRNAs (36) were then cloned into LV-Id1pr/p (Fig. 4A Upper). The effectiveness of the LV-Id1pr/p constructs to drive each shRNAi, following stable integration, was determined using fluorescence and quantitative RT-PCR (Supplementary Fig. S8A, B). Next, WT lineage depleted BM was transduced with Id1pr/p-GFPNS Ω , Id1pr/p-GFPId1 Ω and Id1pr/p-GFPVEGFR2 Ω LV constructs, respectively and transplanted into irradiated WT mice. Tumor growth in Id1pr/p-GFP Id1 Ω and VEGFR2 Ω BMT animals was impaired compared to non-specific control (Fig. 4A lower, B). Notably, Id1pr/p-shRNA-mediated suppression of both Id1 and VEGFR2 resulted in a 2–3 fold reduction of CEPs (Fig. 4C, Supplementary Fig. S9A), but no significant change in CD45⁺/c-kit⁺CD45⁺ hematopoietic cells (Fig. 4C, Supplementary Fig. S9B,C), GR1⁺ neutrophils (Supplementary Fig. S9D), Tie2⁺ monocytes, B220⁺ B-cells,

CD3⁺ T-cells or CD11b⁺ c-kit⁺ myeloid progenitors (Supplementary Fig. S10A–D). Thus indicating the effect of this suppression is CEP specific.

Analysis of tumors also showed a significant reduction in vessel density in Id1pr/p-GFPId1 Ω and Id1pr/p-GFPVEGFR2 Ω BMT mice as compared to control mice (Fig. 4D). RT-PCR analysis of the BM confirmed that Id1 or VEGFR2 shRNA's had indeed suppressed cognate target genes *in vivo*. A 60% reduction in Id1 mRNA was observed in Id1 Ω BM, while a 75% reduction was observed in VEGFR2 mRNA in VEGFR2 Ω BM compared to NS Ω BM. The levels of pan hematopoietic CD45 mRNA also remaining unchanged (Supplementary Fig. S8C). This experiment was not influenced by differential LV transduction efficiency or shRNA-mediated preferential enrichment of specific populations, as the BM of all Id1pr/p-GFP Ω transduced animals showed comparable integrations per cell (Supplementary Fig. S8D). Taken together, these results demonstrate that EPC-intrinsic expression of Id1 and VEGFR2 is critical for effective EPC mobilization from the BM, and for normal tumor vascularization and growth.

Discussion

While the contribution of BM-derived EPCs to tumor neovessel formation has been reported in mice and humans (12,16,37,38), the inability to deliver transgenes specifically to EPCs *in vivo* has precluded the analysis of their biological function, and assessment of their therapeutic potential. In this study we show for the first time using LV Id1 reporter constructs, and Id1^{+/GFP} fluorescent reporter mice (24), that the Id1 gene is selective for EPCs, and can be used to track EPCs in the BM, blood, tumor-stroma, as well as incorporated in tumor vasculature. This identification of lumenally incorporated mature EPCs in the tumor vasculature expressing the Id1 gene, also validates that Id1 marks cells that are true EPCs. Furthermore, this finding validates that EPCs do incorporate into tumor vasculature. To the best of our knowledge this study provides the first direct *in vivo* evidence of EPCs being marked by a single unique marker in each of these tissues.

To confirm the selectivity of Id1 for BM-EPCs, the LV-Id1pr/p construct was used to deliver the suicide transgene HSV-*tk*. Following administration of GCV, EPCs were specifically ablated resulting in a 60–70% reduction in CEPs, as well as angiogenesis inhibition and impaired tumor growth. This Id1 directed specific EPC ablation also did not significantly affect hematopoiesis or other hematopoietic cell populations. These findings are consistent with observations of Id1 knockout mice and their WT littermates, which showed no difference in hematopoietic progenitors (HPCs) (39). Furthermore, although, recent studies have shown that continuous serial transplantation of Id1 knockout BM results (ultimately) in impaired engraft potential (due to a reduction in long term repopulating hematopoietic stem cells/HSCs), Id1 was found to be dispensable for short term recovery of HSCs (24,40). This is supported by the observation in this study that acute suppression of Id1 in the adult BM compartment, while resulting in tumor angiogenic defects was not associated with HSC defects in our HSV-*tk* /GCV treated animals.

The LV-Id1pr/p construct was also designed to express shRNAi designed after an endogenous miRNA and determine the function of endogenous EPC-specific genes, Id1 and VEGFR2 in tumor angiogenesis. ShRNA-mediated suppression of Id1 resulted in EPC mobilization defects (a 70–80% reduction in CEPs), associated with severe angiogenesis inhibition and impaired tumor growth, with no significant change in cells of the hematopoietic lineage (B-cells, T-cells, CD11b⁺ myeloid cells and Tie2⁺ monocytes). This result is consistent with the observations made following the HSV-*tk* delivery in Id1 transgenic mice (14,24). However, our result differs slightly from that of Jankovic *et al.* (40), who reported reduced number of circulating lymphocytes in the PB of resting Id1

knockout mice. Possibly, in our study, acute and short term suppression of Id1 in the BM compartment is devoid of the developmental compensations in the hematopoietic system associated with the Id1 knockout animal. In another study, Lyden *et al.* (14) showed that angiogenesis inhibition in the Id1 mutant was due to defects in mobilization of both VEGFR2⁺ EPCs and VEGFR1⁺ CD11b⁺ hematopoietic cells. However, the use of the combined Id1^{+/-}Id3^{null} genotype in their study may have resulted in defects in VEGFR1⁺ cell mobilization, as a result of Id3 loss; as described (41). Furthermore, we have observed that Id1 silencing (either by shRNAi or in Id1 knockout mice) specifically affects VEGFR2⁺ EPCs, and not VEGFR1⁺ cells (20). In Gao *et al.* (17) we showed that suppression of Id1 in the whole BM by shRNAi leads to EPC and tumor angiogenic defects. In this study, restricted delivery of shRNAi to Id1⁺ expressing cells using the Id1 promoter provides further compelling and direct evidence for the role of Id1 in EPC mobilization in the context of tumor challenge.

Similarly, EPC-specific VEGFR2 knockdown also resulted in loss of EPC function, associated with vessel loss and impaired tumor growth. Notably, administration of VEGFR2 blocking antibody has been previously shown to have anti-angiogenic effects (19), however, anti-VEGFR2 antibody is not specific to EPCs and also recognizes VEGFR2 expressed on endothelial cells in nascent blood vessels (42). Therefore, it has been difficult to discern whether the anti-angiogenic phenotype observed in these studies are due to targeting EPCs, mature vessels or both. Given that VEGFR2 suppression was strictly confined to the EPCs in the BM microenvironment, our results provide the most direct evidence for the role of VEGFR2 in EPC-mediated tumor angiogenesis.

Even though, luminally incorporated BM-derived Id1pr/p⁺ ECs represent a small fraction of the total tumor vasculature, specific ablation demonstrated that EPCs play a critical role in angiogenesis-mediated tumor growth. We have previously shown that tumor recruited EPCs secrete proangiogenic factors (20), suggesting that in addition to providing structural support to nascent vessels EPCs have paracrine function in vessel recruitment. This makes them uniquely important targets for antiangiogenic cancer therapy. However, our results do not discount the perivascular role other tumor recruited BM-derived hematopoietic cells (2,7). Conceivably, each component of the tumor-stroma plays a distinct role in tumor progression, and elimination of specific cell populations may drastically impact tumor growth. Furthermore, variability in reported contribution of EPCs across different mouse tumor models/strains [0% Purhonen *et al.* (21); 2–20% Nolan *et al.* (16); to 90% Lyden *et al.* (14); summarized in review Gao *et al.* (43)], means there is a need for a method to dynamically track and stage EPC involvement. Therefore, given that the role of tumor associated BM-EPCs in cancer progression remains the subject of debate, the selectivity of Id1 for EPCs, and its study through gene manipulation *in vivo*, provides a key tool for further investigation. Furthermore, as the BM-contributes to the tumor microenvironment, LV-delivery of tissue-specific promoters driving RNAi may be used to understand the role of BM-derived cells in tumor biology.

Supplementary Material

Refer to Web version on PubMed Central for supplementary material.

Acknowledgments

We thank Yuri Lazebnik (CSHL) for comments on the manuscript, and Margaret Black (Washington State University) for technical advice on HSV-*tk* experiments. We also thank Raul Cantena (Weill Cornell Medical College), Pamela Moody, Anne Marie Torres (Flow Cytometry Facility, CSHL), Chris Brownlee (Flow Facility, Garvan Institute), Lisa Bianco, Jodi Cobentz, Lea Manzella (Animal Facility, CSHL), and Diane Muller (Zeiss, Australia) for experimental and technical assistance.

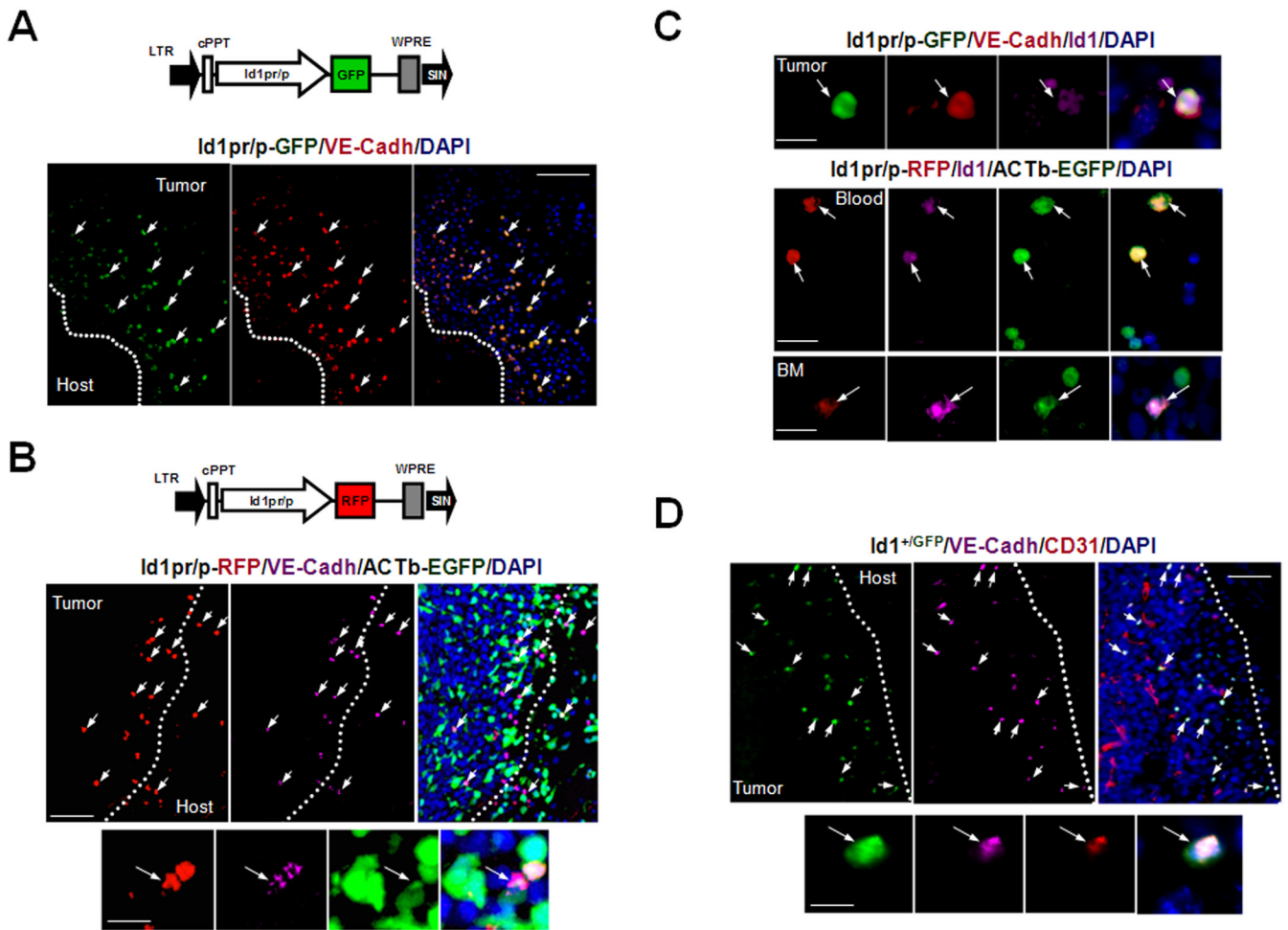
Grant Support: This work was supported by grants held by Vivek Mittal from the National Institutes of Health (www.nih.gov), the Berkowitz Foundation and the Robert I. Goldman foundation, as well as, grants held by Albert Mellick from the Australian Research Council (www.arc.gov.au), the Queensland Cancer Council (www.cancerqld.org.au) and the Griffith Medical Research College, Australia (http://www.qimr.edu.au/research/gmrc/). Alexander Swarbrick is a recipient of a Cancer Institute NSW Early Career Development Fellowship Grant. The funders had no role in study design, data collection and analysis, decision to publish, or preparation of the manuscript.

References

1. Folkman J. Role of angiogenesis in tumor growth and metastasis. *Semin Oncol.* 2002; 29:15–18. [PubMed: 12516034]
2. De Palma M, Venneri MA, Galli R, et al. Tie2 identifies a hematopoietic lineage of proangiogenic monocytes required for tumor vessel formation and a mesenchymal population of pericyte progenitors. *Cancer Cell.* 2005; 8:211–226. [PubMed: 16169466]
3. De Palma M, Mazziere R, Politi LS, et al. Tumor-targeted interferon-alpha delivery by Tie2-expressing monocytes inhibits tumor growth and metastasis. *Cancer Cell.* 2008; 14:299–311. [PubMed: 18835032]
4. Yang L, DeBusk LM, Fukuda K, et al. Expansion of myeloid immune suppressor Gr⁺CD11b⁺ cells in tumor-bearing host directly promotes tumor angiogenesis. *Cancer Cell.* 2004; 6:409–421. [PubMed: 15488763]
5. Marttila-Ichihara F, Auvinen K, Elima K, Jalkanen S, Salmi M. Vascular adhesion protein-1 enhances tumor growth by supporting recruitment of Gr-1+CD11b+ myeloid cells into tumors. *Cancer Res.* 2009; 69:7875–7883. [PubMed: 19789345]
6. Lin EY, Nguyen AV, Russell RG, Pollard JW. Colony-stimulating factor 1 promotes progression of mammary tumors to malignancy. *J Exp Med.* 2001; 193:727–740. [PubMed: 11257139]
7. Pollard JW. Tumour-educated macrophages promote tumour progression and metastasis. *Nat Rev Cancer.* 2004; 4:71–78. [PubMed: 14708027]
8. Coussens LM, Werb Z. Inflammation and cancer. *Nature.* 2002; 420:860–867. [PubMed: 12490959]
9. Nozawa H, Chiu C, Hanahan D. Infiltrating neutrophils mediate the initial angiogenic switch in a mouse model of multistage carcinogenesis. *Proc Natl Acad Sci USA.* 2006; 103:12493–12498. [PubMed: 16891410]
10. Song S, Ewald AJ, Stallcup W, Werb Z, Bergers G. PDGFRbeta+ perivascular progenitor cells in tumours regulate pericyte differentiation and vascular survival. *Nat Cell Biol.* 2005; 27:870–879. [PubMed: 16113679]
11. Kopp HG, Ramos CA, Rafii S. Contribution of endothelial progenitors and proangiogenic hematopoietic cells to vascularization of tumor and ischemic tissue. *Curr Opin Hematol.* 2006; 13:175–181. [PubMed: 16567962]
12. Asahara T, Takahashi T, Masuda H, et al. VEGF contributes to postnatal neovascularization by mobilizing bone marrow derived endothelial progenitor cells. *Embo J.* 1999; 18:3964–3972. [PubMed: 10406801]
13. Urbich C, Dimmeler S. Endothelial progenitor cells: characterization and role in vascular biology. *Circ Res.* 2004; 95:343–353. [PubMed: 15321944]
14. Lyden D, Hattori K, Dias S, et al. Impaired recruitment of bone-marrow derived endothelial and hematopoietic precursor cells blocks tumor angiogenesis and growth. *Nat Med.* 2001; 7:1194–1201. [PubMed: 11689883]
15. Ruzinova MB, Schoer RA, Gerald W, et al. Effect of angiogenesis inhibition by Id loss and the contribution of bone-marrow-derived endothelial cells in spontaneous murine tumors. *Cancer Cell.* 2003; 4:277–289. [PubMed: 14585355]
16. Nolan DJ, Ciarrocchi A, Mellick AS, et al. Bone marrow-derived endothelial progenitor cells are a major determinant of nascent tumor neovascularization. *Genes Dev.* 2007; 21:1546–1558. [PubMed: 17575055]
17. Gao D, Nolan DJ, Mellick AS, et al. EPCs control the angiogenic switch in mouse lung metastasis. *Science.* 2008; 319:195–198. [PubMed: 18187653]

18. Bertolini F, Shaked Y, Mancuso P, Kerbel RS. The multifaceted circulating endothelial cell in cancer: towards marker and target identification. *Nat Rev Cancer*. 2006; 6:835–845. [PubMed: 17036040]
19. Shaked Y, Ciarrocchi A, Franco M, et al. Therapy-induced acute recruitment of circulating endothelial progenitor cells to tumors. *Science*. 2006; 313:1785–1787. [PubMed: 16990548]
20. Gao D, Mittal V. The role of bone-marrow-derived cells in tumor growth, metastasis initiation and progression. *Trends Mol Med*. 2009; 15:333–343. [PubMed: 19665928]
21. Purhonen S, Palm J, Rossi D, et al. Bone marrow-derived circulating endothelial precursors do not contribute to vascular endothelium and are not needed for tumor growth. *Proc Natl Acad Sci USA*. 2008; 105:6620–6625. [PubMed: 18443294]
22. Perk J, Gil-Bazo I, Chin Y, et al. Reassessment of id1 protein expression in human mammary, prostate, and bladder cancers using a monospecific rabbit monoclonal anti-id1 antibody. *Cancer Res*. 2006; 66:10870–10877. [PubMed: 17108123]
23. Lyden D, Young AZ, Zagzag D, et al. Id1 and Id3 are required for neurogenesis, angiogenesis and vascularization of tumour xenografts. *Nature*. 1999; 401:670–677. [PubMed: 10537105]
24. Perry SS, Zhao Y, Nie L, et al. Id1, but not Id3, directs long-term repopulating hematopoietic stem-cell maintenance. *Blood*. 2007; 110:2351–2360. [PubMed: 17622570]
25. Okabe M, Ikawa M, Kominami K, Nakanishi T, Nishimune Y. 'Green mice' as a source of ubiquitous green cells. *FEBS Lett*. 1997; 407:313–319. [PubMed: 9175875]
26. Tudor KS, Deem TL, Cook-Mills JM. Novel alpha 4-integrin ligands on an endothelial cell line. *Biochem Cell Biol*. 2000; 78:99–113. [PubMed: 10874471]
27. Kumar R, Conklin DS, Mittal V. High-throughput selection of effective RNAi probes for gene silencing. *Genome Res*. 2003; 13:2333–2340. [PubMed: 14525931]
28. Rose-Meyer RB, Mellick AS, Garnham BG, et al. The measurement of adenosine and estrogen receptor expression in rat brains following ovariectomy using quantitative PCR analysis. *Brain Res Brain Res Protoc*. 2003; 11:9–18. [PubMed: 12697258]
29. Campbell RE, Tour O, Palmer AE, et al. A monomeric red fluorescent protein. *Proc Natl Acad Sci USA*. 2002; 99:7877–7882. [PubMed: 12060735]
30. Salmon P, Kindler V, Ducrey O, et al. High-level transgene expression in human hematopoietic progenitors and differentiated blood lineages after transduction with improved lentiviral vectors. *Blood*. 2000; 96:3392–3398. [PubMed: 11071633]
31. Perfetto SP, Chattopadhyay PK, Roederer M. Seventeen-colour flow cytometry: unravelling the immune system. *Nat Rev Immunol*. 2004; 4:648–655. [PubMed: 15286731]
32. Katagiri T, Imada M, Yanai T, et al. Identification of a BMP-responsive element in Id1, the gene for inhibition of myogenesis. *Genes Cells*. 2002; 7:949–960. [PubMed: 12296825]
33. Magalhaes GS, Muotri AR, Marchetto MC, Menck CF, Ventura AM. An adenovirus vector containing the suicide gene thymidine kinase for a broad application in cancer gene therapy. *Mem Inst Oswaldo Cruz*. 2002; 97:547–552. [PubMed: 12118289]
34. Lalor PA, Mapp PI, Hall PA, Revell PA. Proliferative activity of cells in the synovium as demonstrated by a monoclonal antibody, Ki67. *Rheumatol Int*. 1987; 7:183–186. [PubMed: 3321379]
35. Osti D, Marras E, Ceriani I, et al. Comparative analysis of molecular strategies attenuating positional effects in lentiviral vectors carrying multiple genes. *Virology*. 2006; 346:93–101.
36. Dickins RA, Hemann MT, Zilfou JT, et al. Probing tumor phenotypes using stable and regulated synthetic microRNA precursors. *Nat Genet*. 2005; 11:1289–1295. [PubMed: 16200064]
37. Peters BA, Diaz LA, Polyak K, et al. Contribution of bone marrow-derived endothelial cells to human tumor vasculature. *Nat Med*. 2005; 11:261–262. [PubMed: 15723071]
38. Duda DG, Cohen KS, Kozin SV, et al. Evidence for incorporation of bone marrow-derived endothelial cells into perfused blood vessels in tumors. *Blood*. 2006; 107:2774–2776. [PubMed: 16339405]
39. Yan W, Young AZ, Soares VC, et al. High incidence of T-cell tumors in E2A-null mice and E2A/Id1 double-knockout mice. *Mol Cell Biol*. 1997; 12:7317–7327. [PubMed: 9372963]

40. Jankovic V, Ciarrocchi A, Boccuni P, et al. Id1 restrains myeloid commitment, maintaining the self-renewal capacity of hematopoietic stem cells. *Proc Natl Acad Sci U S A.* 2007; 104:1260–1265. [PubMed: 17227850]
41. Kaplan RN, Riba RD, Zacharoulis S, et al. VEGFR1-positive haematopoietic bone marrow progenitors initiate the pre-metastatic niche. *Nature.* 2005; 438:820–827. [PubMed: 16341007]
42. Shibuya M. Differential roles of vascular endothelial growth factor receptor-1 and receptor-2 in angiogenesis. *J Biochem Mol Biol.* 2006; 39:469–478. [PubMed: 17002866]
43. Gao D, Nolan D, McDonnell K, et al. Bone marrow-derived endothelial progenitor cells contribute to the angiogenic switch in tumor growth and metastatic progression. *Biochim Biophys Acta.* 2009; 1796:33–40. [PubMed: 19460418]

**Figure 1.**

Id1 Marks EPCs in the PB, BM and Tumor-Stroma. A Upper, Schematic of Id1pr/p-GFP LV vector: Id1pr/p driving GFP expression. cPPT, central polyurine tract; WPRE, woodchuck hepatitis virus post transcription regulatory element; LTR, long terminal repeat; SIN, self inactivating. Lower, Microscopy showing recruitment of Id1pr/p-GFP⁺ cells to early nonvascularized LLC tumor periphery (arrows, day 8, n=15) in Id1pr/p-GFP BMT mice. Scale bar, 50 μm. B Upper, Schematic of Id1pr/p-RFP LV vector: Id1pr/p driving monomeric RFP/ mCherryTM expression. Lower, Microscopy showing recruitment of Id1pr/p-RFP⁺ cells to early nonvascularized LLC tumor periphery (arrows, day 8, n=15) in Id1pr/p-RFP/ACTb-EGFP BMT mice. Scale bar, 50 μm. High resolution (63×) image showing the Id1pr/p-RFP⁺ can be used to mark and distinguish BM-derived ACTb-EGFP⁺ VE-Cadherin⁺ BM-EPCs (arrow) from other BM cells in within the tumor-stroma. Scale bar, 10 μm. C top, Image showing that the LV-Id1pr/p-GFP construct can be used to mark Id1 protein expressing VE-cadherin⁺ BM-EPCs (arrow) in the tumor stroma. Bar, 10 μm. Bottom, high-resolution (×63) microscopic images of cytopun BM and PB from LLC tumor-challenged ACTb-EGFP/Id1pr/p-RFP BMT animals, showing that Id1pr/p⁺ EPCs in the BM and PB express nuclear Id1 protein (white arrows). Bar, 20 μm. D Upper, Microscopy showing vasculature and BM-derived Id1⁺/GFP⁺ VE-Cadherin⁺ CD31^{low} BM-EPCs as part of the tumor-stroma (arrows) of LLC tumors (day 15) implanted into Id1⁺/GFP⁺ BMT mice (n=10). Scale bar, 50 μm. Lower, High resolution (63×) of BM-derived Id1⁺/GFP⁺

VE-Cadherin⁺ CD31^{low} BM-EPC (arrow) in the tumor-stroma of LLC tumors (day 15) implanted into Id1^{+/GFP+} BMT mice. Scale bar, 10 μ m.

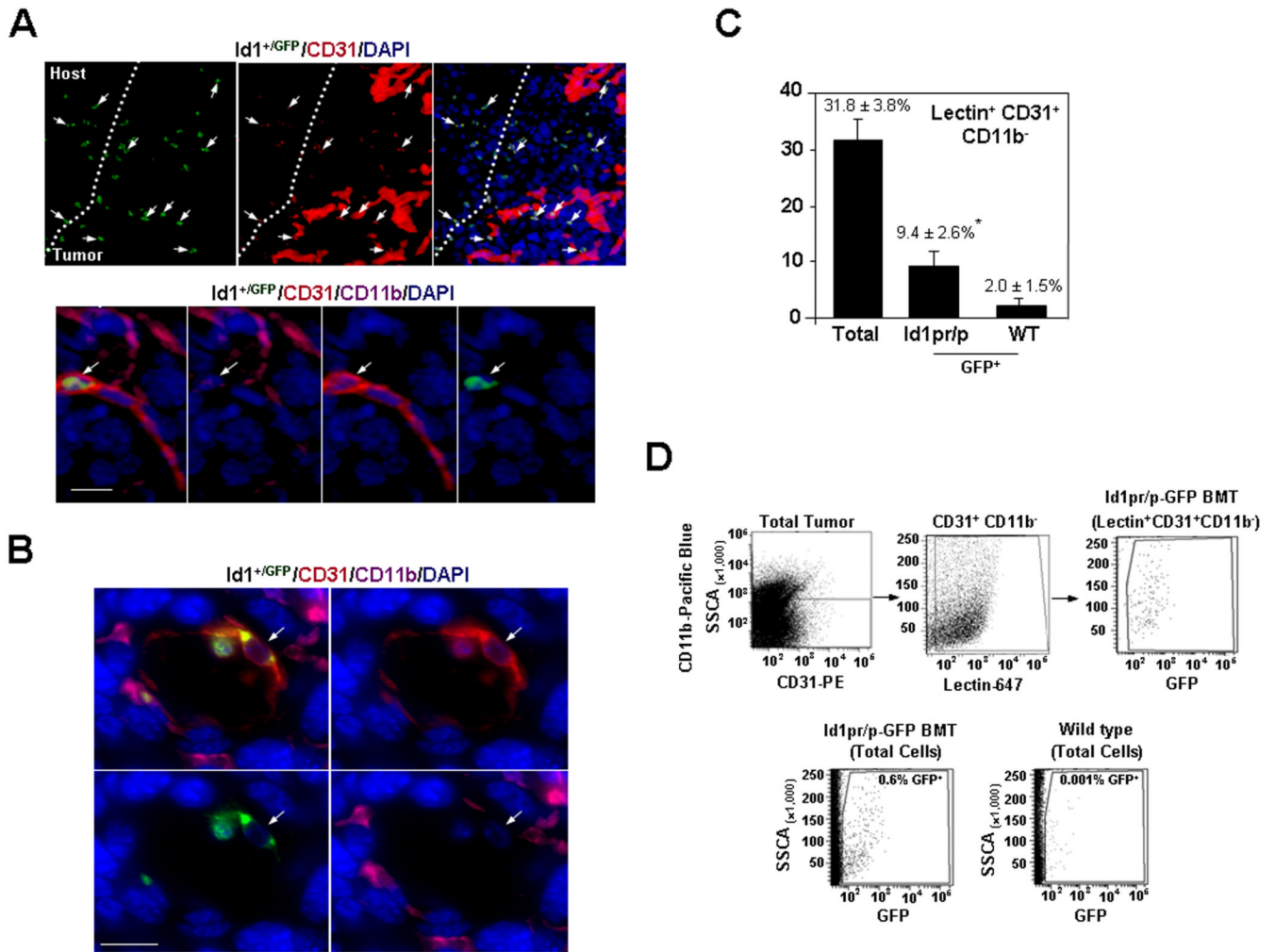


Figure 2.

Id1 Marks Luminally Incorporated, Mature EPCs in the Nascent Tumor Vasculature. A Upper, Microscopy showing vasculature and BM-derived Id1^{+/GFP} CD31^{low} CD11b⁻ BM-EPCs as part of the tumor-stroma (arrows) of LLC tumors (day 15) implanted into Id1^{+/GFP} BMT mice (n=10). Scale bar, 50 μ m. Lower, Microscopy of a tumor vessel showing an incorporated BM-derived mature EPC (Id1^{+/GFP} CD31⁺ CD11b⁻, arrow) in LLC tumors (day 15) implanted into Id1^{+/GFP} BMT mice. Scale bar, 20 μ m. B, High resolution (63 \times) transverse immunofluorescent image of tumor vessel showing an incorporated BM-derived mature EPC (Id1^{+/GFP} CD31⁺ CD11b⁻, arrow) in LLC tumors (day 15) implanted into Id1^{+/GFP} BMT mice. Scale bar, 20 μ m. C, Summary of FACS analysis showing contribution of Id1⁺ mature EPCs in functional vessels, by Isolectin staining in LLC tumor (day 6) in Id1pr/p-GFP BMT mice. D, Representative scatter plots showing derivation of GFP gates. SSCA, side scatter values.

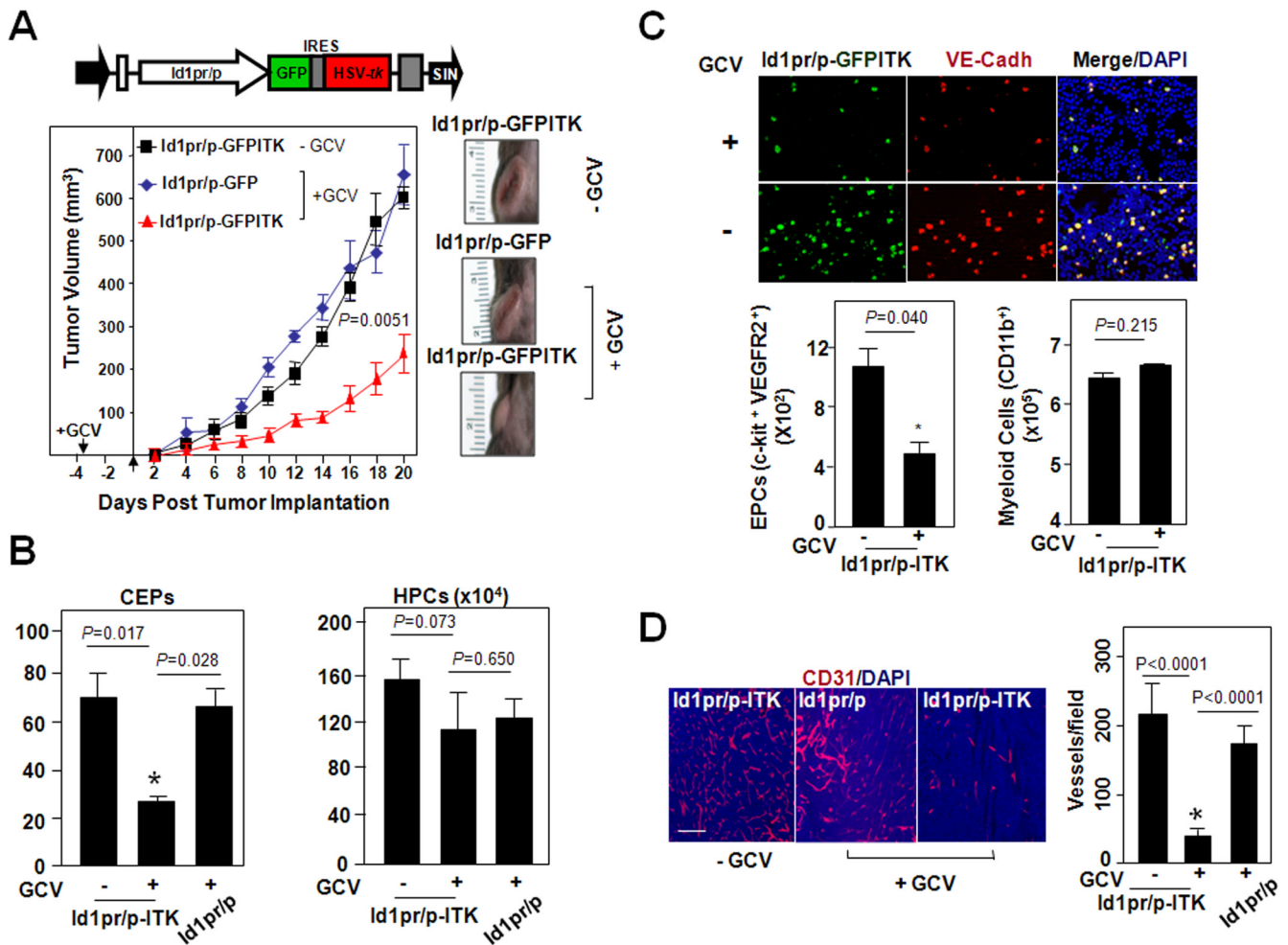


Figure 3. Selective Elimination of Id1pr/p⁺ EPCs by Delivery of a Suicide Gene HSV-tk Impairs Tumor Growth. **A** Upper, Schematic of Id1pr/p LV vector, with Id1pr/p driving GFP and HSV-tk expression. Lower, LLC tumor growth (Mean±S.E.M) and morphology in Id1pr/p-GFPITK BMT mice (n=10) and Id1pr/p-GFP BMT mice (n=5), either treated with GCV (+GCV) or untreated (-GCV). Similar trends observed in repeat experiment. **B**, FACS analysis of PB from tumor challenged Id1pr/p-GFPITK (+GCV), Id1pr/p-GFPITK (-GCV), and GCV control Id1pr/p-GFP (+GCV) BMT mice, showing number of mobilized CEPs (c-kit⁺ VEGFR2⁺) and HPCs (c-kit⁺ CD45⁺). A total of 1×10⁶ cells were analyzed per animal. Data is represented as mean number of cells per 1×10⁵ PBMCs±S.E.M (n=5 per group); analyzed by Students t-test. **C** Upper, Microscopic analysis of EPCs (VE-Cadherin⁺ GFP⁺) from the BM following GCV treatment in Id1pr/p-GFPITK BMT mice. Lower, FACS analysis of the BM from tumor challenged Id1pr/p-GFPITK (- or + GCV) BMT mice, showing the number of EPCs (c-kit⁺ VEGFR2⁺), myeloid cells (CD11b⁺). Data showing significant difference between GCV treated Id1pr/p-GFPITK and untreated animals (P=0.040, by Students t-Test). Numbers are normalized per 1×10⁶ BM mononuclear cells. **D**, CD31⁺ immunostaining showing a lower vessel density in Id1pr/p-GFPITK +GCV LLC tumors in comparison to Id1pr/p-GFPITK -GCV and Id1pr/p LLC tumors (n=15), Scale bar, 100µm. Data represented as average number of vessels per field±S.E.M. and analyzed by Students t-test.

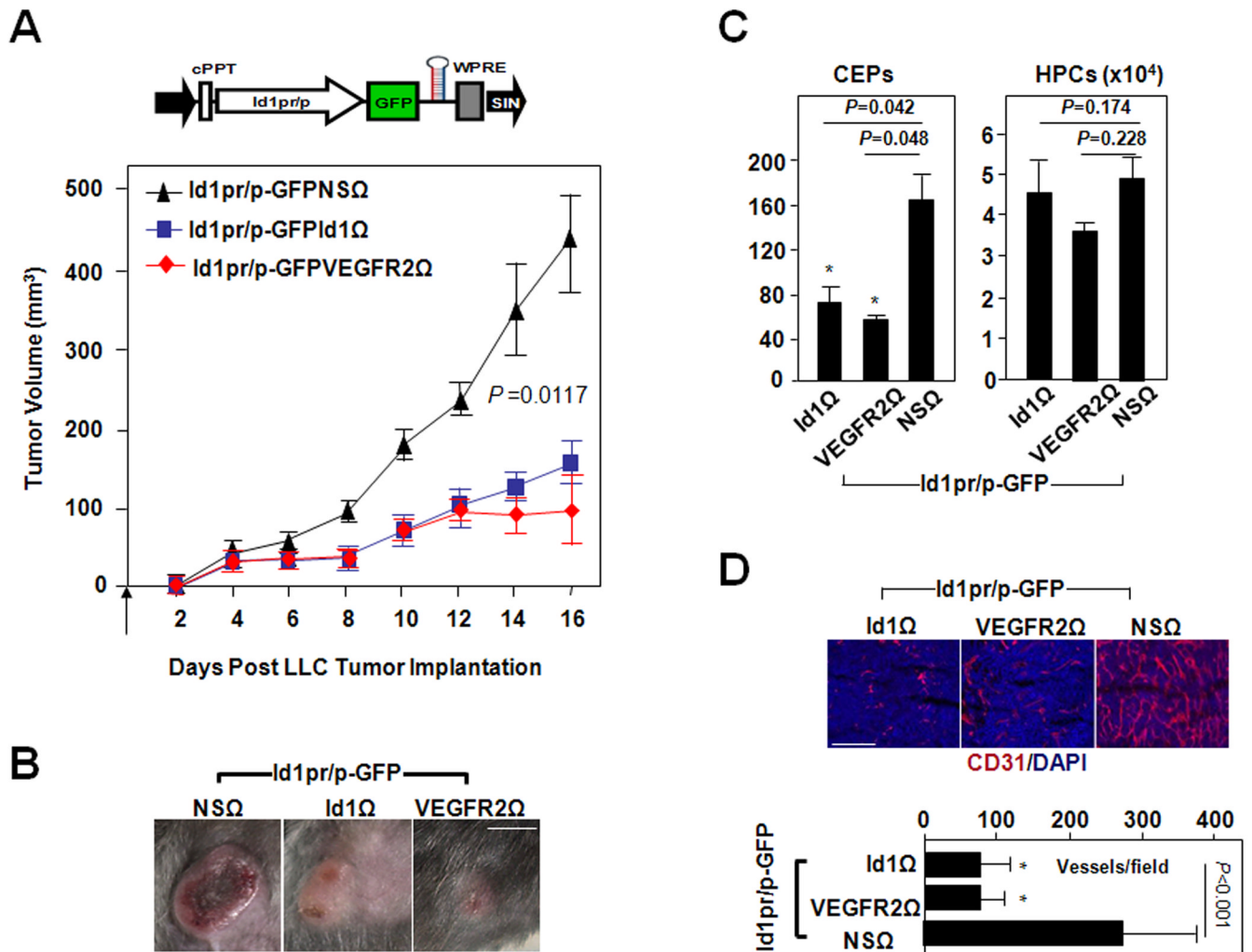


Figure 4.

Id1pr/p shRNA-Mediated Suppression of VEGFR2 and Id1 in the EPCs Results in Angiogenesis Inhibition and Impaired Tumor Growth. A Upper, Schematic of Id1pr/p-GFPΩ LV vector with Id1 promoter driving GFP and miR30-based Ω expression. Lower, LLC tumor growth in Id1pr/p-GFPNSΩ, Id1pr/p-GFPId1Ω and Id1pr/p-GFPVEGFR2Ω BMT mice. Data represented as mean volume±S.E.M ($P=0.0117$ by Student's t-Test, $n=5$ per group). B, LLC tumor morphology in Id1pr/p-GFPNSΩ, Id1pr/p-GFPId1Ω and Id1pr/p-GFPVEGFR2Ω BMT mice, Scale bar, 5mm. C, FACS analysis of PB showing number of CEPs (c-kit⁺ VEGFR2⁺), and HPCs (c-kit⁺CD45⁺) from LLC tumor challenged Id1pr/p-GFPΩ mice. Data is represented as mean number of cells per $1 \times 10^5 \pm$ S.E.M. ($n=5$ per group; P values, by Student's t-Test). This experiment was repeated, similar trends observed. D, CD31⁺ immunostaining showing a higher vessel density in Id1pr/p-GFPNSΩ LLC tumors in comparison to Id1pr/p-GFPId1Ω and Id1pr/p-GFPVEGFR2Ω LLC tumors ($n=15$), Scale bar, 100μm. Data represented as average number of vessels per field±S.E.M. and analyzed by Student's t-test.